Raf-mediated cardiac hypertrophy in adult *Drosophila*

Lin Yu[1], Joseph Daniels[1], Alex E. Glaser[1] and Matthew J. Wolf[1,*]

SUMMARY

In response to stress and extracellular signals, the heart undergoes a process called cardiac hypertrophy during which cardiomyocytes increase in size. If untreated, cardiac hypertrophy can progress to overt heart failure that causes significant morbidity and mortality. The identification of molecular signals that cause or modify cardiomyopathies is necessary to understand how the normal heart progresses to cardiac hypertrophy and heart failure. Receptor tyrosine kinase (RTK) signaling is essential for normal human cardiac function, and the inhibition of RTKs can cause dilated cardiomyopathies. However, neither investigations of activated RTK signaling pathways nor the characterization of hypertrophic cardiomyopathy in the adult fly heart has been previously described. Therefore, we developed strategies using *Drosophila* as a model to circumvent some of the complexities associated with mammalian models of cardiovascular disease. Transgenes encoding activated EGFR^{A887T}, Ras85D^{V12} and Ras85D^{V12S35}, which preferentially signal to Raf, or constitutively active human or fly Raf caused hypertrophic cardiomyopathy as determined by decreased end diastolic lumen dimensions, abnormal cardiomyocyte fiber morphology and increased heart wall thicknesses. There were no changes in cardiomyocyte cell numbers. Additionally, activated Raf also induced an increase in cardiomyocyte ploidy compared with control hearts. However, preventing increases in cardiomyocyte ploidy using *fizzy-related* (*Fzr*) RNAi did not rescue Raf-mediated cardiac hypertrophy, suggesting that Raf-mediated polyploidization is not required for cardiac hypertrophy. Similar to mammals, the cardiac-specific expression of RNAi directed against *MEK* or *ERK* rescued Raf-mediated cardiac hypertrophy. However, the cardiac-specific expression of activated ERK^{D334N}, which promotes hyperplasia in non-cardiac tissues, did not cause myocyte hypertrophy. These results suggest that ERK is necessary, but not sufficient, for Raf-mediated cardiac hypertrophy.

INTRODUCTION

Cardiomyopathies are generally associated with a myocyte growth program that leads to an increase in the size of individual muscle cells. Individuals who have cardiac hypertrophy and cardiomyopathies are predisposed to the development of heart failure (Vasan et al., 1997). Heart failure affects 5.7 million individuals in the United States, has an annual economic health care burden in excess of US$34 billion in the United States, is associated with significant morbidity and has a 5-year mortality rate of ~50% despite current pharmacological and device-based therapies (Roger et al., 2010). Furthermore, the development of new pharmaceutical agents to treat heart failure has been disappointing despite an increased understanding of the pathophysiology of cardiomyopathies.

Since the initial descriptions of cardiac hypertrophy in humans, substantial efforts have been directed towards understanding the underlying molecular mechanisms. In response to a variety of stimuli, including RTK-mediated signals, the mammalian heart undergoes morphological changes that contribute to the development of dilated or hypertrophic cardiomyopathies (Heineke and Molkentin, 2006). Dilated cardiomyopathies are characterized by enlargement of the heart chambers, thinning of the heart walls and poor contractility of the myocardium (Braunwald and Bonow,

2012). These changes are manifest as enlargements of chamber dimensions during diastole, when the heart is relaxed, and systole, when the heart is contracted, resulting in systolic dysfunction. In fact, the thinning of the heart walls can result from a process called 'eccentric hypertrophy' in which sarcomeres are added in series (Braunwald and Bonow, 2012). Hypertrophic cardiomyopathies are characterized by 'a thickened but nondilated left ventricle' (Braunwald and Bonow, 2012). The thickened heart wall in cardiac hypertrophy can occur by the addition of sarcomeres in parallel or by a process whereby the normal architecture of the myocardium becomes disarrayed. As a result, the end-diastolic chamber dimensions are normal or reduced, and systolic function is preserved until overt heart failure develops.

The inhibition of RTKs in the mammalian heart contributes to the development of dilated cardiomyopathies in which the heart chamber becomes enlarged and poorly contractile (Crone et al., 2002). In fact, individuals who receive certain chemotherapy antagonists directed towards RTKs are predisposed to developing dilated cardiomyopathy and heart failure (Chen et al., 2008; Chu et al., 2007; Suter et al., 2007). Conversely, mutations that cause inappropriate activation of RTKs and downstream signaling molecules – such as the small GTP-ase Ras and the serine/threonine-specific protein kinase Raf – are associated with a variety of human syndromes, including Noonan syndrome (Gelb and Tartaglia, 2011; Pandit et al., 2007). Moreover, subsets of individuals with Noonan syndrome that have activating mutations in Raf are predisposed to hypertrophic cardiomyopathy (Pandit et al., 2007). Therefore, identifying the signals that cause cardiac hypertrophy can lead to new insights into the pathophysiology of this disease.

Strategies using the fruit fly, *Drosophila melanogaster*, have been developed to facilitate the discovery of genes that cause cardiomyopathies. The adult fly heart is a contractile tube that is a single myocyte layer thick and is composed of pairs of

[1]Duke University Medical Center, 321 Sands Building, Research Drive, Durham, NC 27710, USA
*Author for correspondence (wolf0008@mc.duke.edu)

TRANSLATIONAL IMPACT

Clinical issue

Cardiac hypertrophy is a common condition that is triggered by environmental or genetic cues in which the heart muscle enlarges because of an increase in the size of cardiomyocytes. If untreated, cardiac hypertrophy can progress to heart failure and sudden cardiac death. Since the initial descriptions of cardiac hypertrophy in humans, substantial efforts have been directed towards understanding the molecular mechanisms that underlie this condition. Thus, abnormalities in receptor tyrosine kinase (RTK)-mediated signals and downstream signaling molecules are now known to contribute to some forms of cardiac hypertrophy. In addition, specific activating mutations in human Raf, a serine/threonine-specific protein kinase, have been associated with the development of cardiac hypertrophy in subsets of individuals who have Noonan syndrome, a genetic developmental disorder characterized by short stature, specific facial features and congenital heart defects. However, to understand how the normal heart progresses to cardiac hypertrophy and heart failure, the molecular signaling pathways and gene expression programs that together control the growth and differentiation of cardiomyocytes need to be studied in depth.

Results

In this study, the authors provide the first description of cardiac hypertrophy and the signaling pathways controlling its development in adult *Drosophila*. Using optical coherence tomography (a method that produces images of the heart in intact live flies, similar to echocardiography in humans), confocal microscopy and histological analysis, the authors show that fly cardiomyocytes become enlarged and the volume of cardiac lumen decreases in response to the cardiac-specific expression of signals that emanate from EGFR through Ras, Raf, MEK and ERK. These findings recapitulate aspects of cardiac hypertrophy that are generally observed in mammals. Moreover, cardiac hypertrophy seems to be independent of increases in cardiomyocyte DNA content, an association that has been observed in human cardiac hypertrophy.

Implications and future directions

These results serve as a proof-of-principle that the *Drosophila* heart can undergo cardiac hypertrophy similar to humans in response to molecular signals. Thus, these findings establish the *Drosophila* model of cardiac hypertrophy as a platform for the identification of signaling molecules that cause or modify the development of cardiovascular disease. These signaling molecules could eventually provide new therapeutic targets for the treatment of heart failure.

cardiomyocytes with circumferentially oriented myofibers (Wolf, 2012; Wolf and Rockman, 2011). Although the fly heart is undoubtedly less complex in structure compared with the mammalian heart, many signaling pathways that control myocyte growth and function are highly conserved among flies and mammals (Bodmer and Venkatesh, 1998; Wolf and Rockman, 2011). The simplicity of the fly heart, in conjunction with the vast resources available to readily manipulate the fly genome and signaling pathways, provides unique opportunities to examine how signaling molecules affect cardiomyocyte morphology and growth. As a genetically tractable system, the fly can serve as a platform for the discovery of molecules involved in myocyte biology and as a model to validate human gene mutations associated with disease syndromes.

Previously, we reported the results of a screen that identified mutants causing dilated cardiomyopathies in the fruit fly (Yu et al., 2010). Using optical coherence tomography (OCT) to measure the end-diastolic dimensions (EDDs) and end-systolic dimensions (ESDs), when the heart is fully relaxed or contracted, respectively, we identified flies that had enlarged hearts due to mutations in a

Rhomboid protease. Rhomboid protease performs a crucial step in the processing of a fly ortholog of the EGFR ligand, Spitz, and the expression of soluble forms of Spitz rescued the cardiac abnormalities associated with Rhomboid deficiencies (Yu et al., 2010). Moreover, the cardiac-specific expression of dominant-negative EGFR caused a progressive dilated cardiomyopathy in adult flies, suggesting that EGFR-mediated signals in the *Drosophila* heart recapitulates abnormalities observed in mammals, including humans.

Dilated heart phenotypes in the fly have been well described; however, the characterization of hypertrophic heart phenotypes in *Drosophila* has been limited. Using multiple approaches, including OCT, confocal microscopy and histological analyses of heart wall thicknesses, we identify that the activation of EGFR and the downstream molecules Ras and Raf causes a reduction in cardiac lumen sizes at end-diastole and an increase in heart wall thicknesses in adult *Drosophila*. Furthermore, the changes in heart wall thicknesses are due to myocyte hypertrophy: cardiomyocyte cell number was unchanged. We also show that the cardiac-specific expression of RNAi directed against *mitogen-activated protein kinase kinase* (*MEK*) or *extracellular signal-regulated kinase* (*ERK*) rescue Raf-mediated cardiac hypertrophy. However, the cardiac-specific activation of ERK does not cause cardiac hypertrophy. This suggests that additional ERK-independent signals emanating from Raf might contribute to hypertrophic cardiomyopathy. In addition, activated Raf induced an increase in cardiomyocyte ploidy compared with that seen in control hearts. However, preventing increases in cardiomyocyte ploidy using *fizzy-related* (*Fzr*) RNAi did not rescue Raf-mediated cardiac hypertrophy, suggesting that Raf-mediated polyploidization is not required for cardiac hypertrophy. Collectively, these results demonstrate that the fly can recapitulate aspects of hypertrophic cardiomyopathy that are seen in mammals and can serve as a platform for the discovery of novel signals that mediate cardiac hypertrophy.

RESULTS

Activated EGFR or Ras causes cardiac hypertrophy in adult flies

RTKs, including EGFR, are necessary to maintain cardiac function in mammals and flies (Heineke and Molkentin, 2006). Previously, we identified that the inhibition of EGFR caused dilated heart chambers in adult flies (Yu et al., 2010). Because the effects on cardiac function of signaling molecules that are downstream from EGFR have not been evaluated in the adult fly, we examined the effects of EGFR-mediated signaling in the adult fly heart. The *tinC*-mediated, cardiac-specific expression of constitutively activated $EGFR^{A887T}$ (designated $EGFR^{Act}$) or the downstream GTPase $Ras85D^{V12}$ resulted in significantly decreased frequencies of eclosion and poor survival of adult escapers (supplementary material Fig. S1A and data not shown). The embryonic dorsal vessels in $tinC>EGFR^{Act}$ heterozygous flies were similar to controls, but the pupal heart in $tinC>EGFR^{Act}$ flies in both eclosers and non-eclosers developed similar morphological abnormalities to each other, consistent with the effects on cardiac remodeling during pupal morphogenesis (supplementary material Fig. S1B; Fig. S2).

Adult $tinC>EGFR^{Act}$ and $tinC>Ras85D^{V12}$ heterozygote flies had smaller heart chambers with reduced EDDs compared with controls, as measured by OCT [EDD 95.6±2.9 μm for *tinC-Gal4* driver alone (controls) versus 36.4±6.0 μm for $tinC>EGFR^{Act}$ or

32.3±5.9 µm for *tinC>Ras85D^{V12}*, *P*<0.05; Fig. 1A,B; supplementary material Table S1]. Histological analyses of cardiac chambers from adult *tinC>EGFR^{Act}* and *tinC>Ras85D^{V12}* heterozygous flies showed heart wall thicknesses that were increased two- to three-times compared with controls (6.7±0.6 µm for controls versus 15.2±0.1

µm for *tinC>EGFR^{Act}* versus 23.1±1.0 µm for *tinC>Ras85D^{V12}*, *P*<0.05; Fig. 1C,D). To examine the cardiomyocyte architecture in more detail and to avoid obscuration of the heart by the closely attached non-cardiac dorsal diaphragm (also known as the ventral longitudinal muscle), we generated transgenic flies harboring GFP
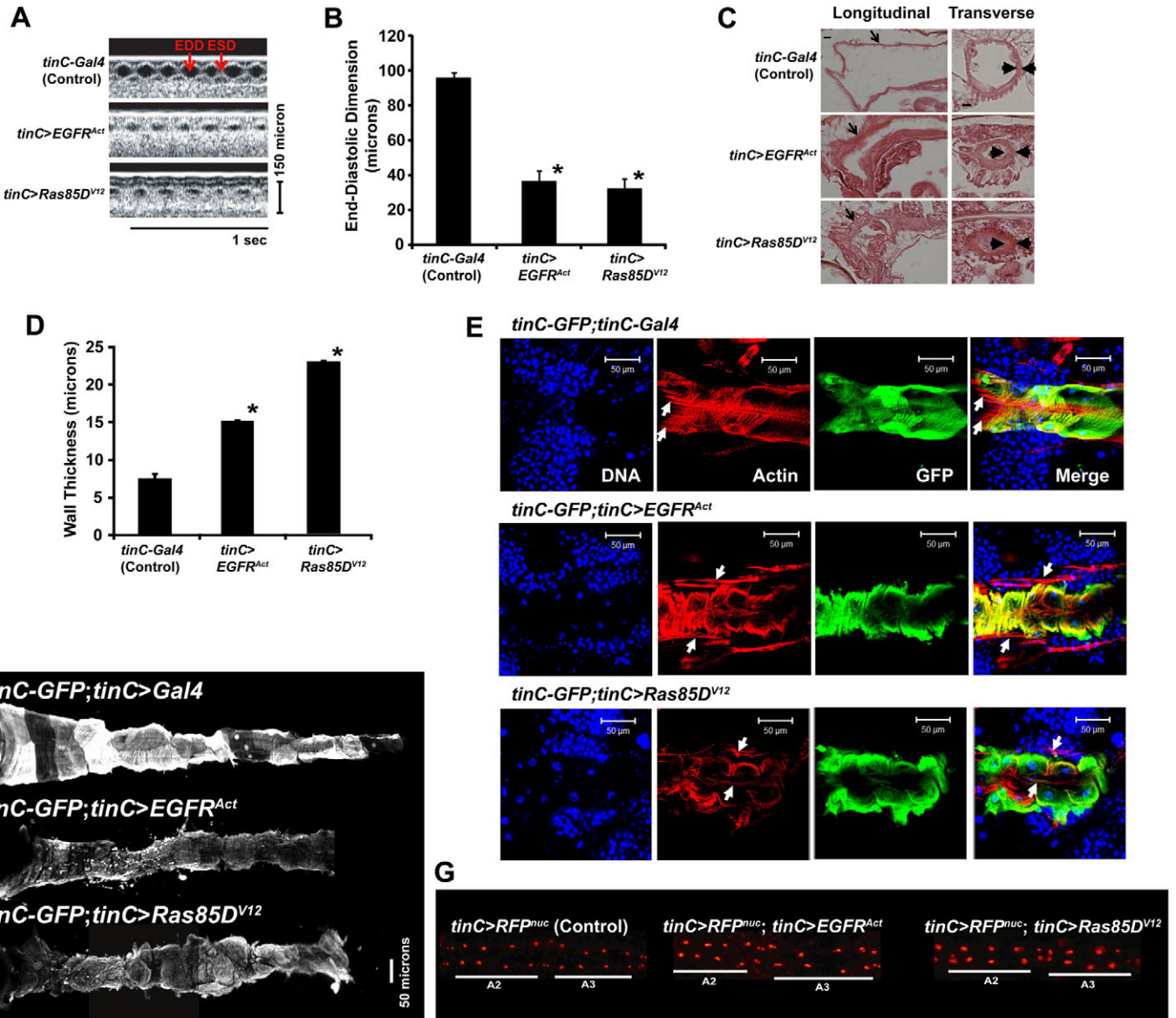

Fig. 1. The cardiac-specific expression of activated EGFR or Ras85D causes hypertrophy. (A) OCT M-mode images of the heart lumen from *tinC-Gal4* driver control, *tinC>EGFR^{Act}* and *tinC>Ras85D^{Act}* adult flies. A 1-second marker and 150 µm standard are shown. (B) Summary data for OCT measurements of EDDs for *tinC-Gal4* driver control, *tinC>EGFR^{Act}* and *tinC>Ras85D^{Act}* adult flies. Ten to twelve flies per group. **P*<0.05 for indicated transgenic fly line versus control. (C) Histological sections in longitudinal and transverse orientations showing heart wall thicknesses in the first and second abdominal segments (A1/A2) from *tinC-Gal4* driver control, *tinC>EGFR^{Act}* and *tinC>Ras85D^{Act}* adult flies. Arrows indicate heart walls; arrowheads indicate heart wall thicknesses. Scale bar: 10 µm. (D) Summary data for heart wall thicknesses measured from serial transverse histological sections from *tinC-Gal4* driver control, *tinC>EGFR^{Act}* and *tinC>Ras85D^{Act}* adult flies. **P*<0.05 for indicated transgenic fly line vs control. Three to six flies per group. (E) Confocal microscopy of *tinC-GFP; tinC-Gal4* adult fly heart, *tinC>EGFR^{Act}* adult fly heart, and *tinC>Ras85D^{Act}* adult fly heart from the A1/A2 abdominal segments. GFP imaging (green) and phalloidin staining of actin (red) show the circumferentially oriented fibers of the adult heart. Ventral longitudinal muscle fibers (also known as the dorsal diaphragm), which do not express *tinC-GFP*, are also seen by staining with Texas-Red–phalloidin (red) (denoted by arrows). TO-PRO-3 was used for DNA staining (blue). (F) Confocal microscopy with *z*-stack reconstructions showing the abnormal circumferentially oriented heart myofibers in *tinC-GFP; tinC>EGFR^{Act}* and *tinC-GFP; tinC>Ras85D^{Act}* flies compared with *tinC-GFP; tinC-Gal4* controls. (G) Fluorescent imaging of nuclear-localized RFP in hearts from *tinC>RFP^{nuc}* control, *tinC>RFP^{nuc}; tinC>EGFR^{Act}* and *tinC>RFP^{nuc}; tinC>Ras85D^{V12}* flies. The A2 and A3 abdominal segments are shown. Note that all flies in this figure and following figures were heterozygous for the indicated transgenes.
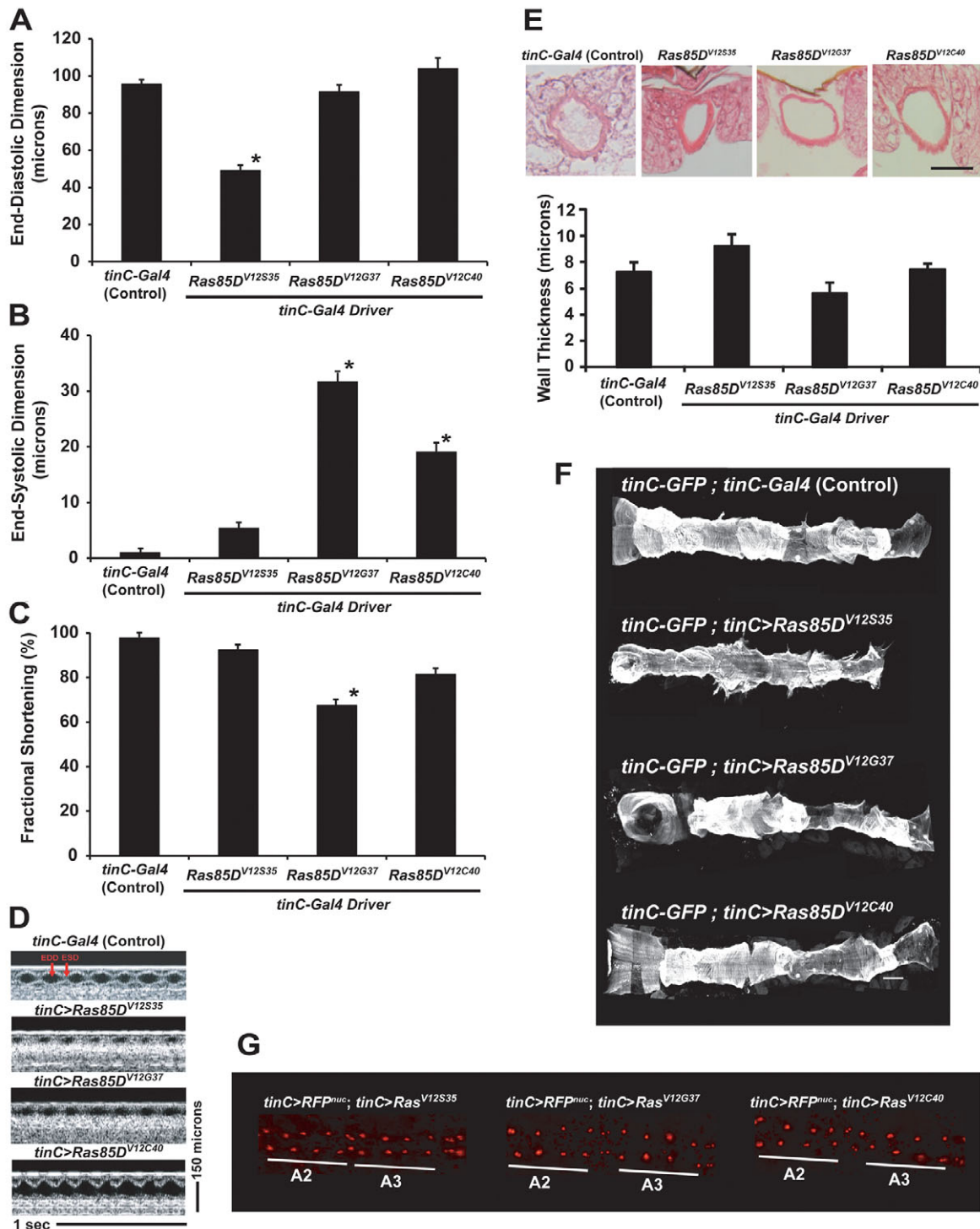
Fig. 2. The expression of Ras85D^{V12S35}, but not Ras85D^{V12G37} or Ras85D^{V12C40}, causes cardiac hypertrophy. Summary data for OCT measurements of EDD (A), ESD (B) and FS (C) for *tinC-Gal4* driver control (*n*=18), *tinC>Ras85D^{V12S35}* (*n*=11), *tinC>Ras85D^{V12G37}* (*n*=16) and *tinC>Ras85D^{V12C40}* (*n*=12) adult flies. *$P<0.05$ for indicated transgenic fly line vs control. (D) Representative M-mode OCT images for *tinC-Gal4* driver control, *tinC>Ras85D^{V12S35}*, *tinC>Ras85D^{V12G37}* and *tinC>Ras85D^{V12C40}* adult flies. A 1-second marker and 150 µm standard are shown. (E) Histological sections in transverse orientation showing heart wall thicknesses in the A1/A2 segments from *tinC-Gal4* driver control (*n*=10), *tinC>Ras85D^{V12S35}* (*n*=11), *tinC>Ras85D^{V12G37}* (*n*=10) and *tinC>Ras85D^{V12C40}* (*n*=8) adult flies (top) and summary data of wall thicknesses (bottom). (F) Confocal microscopy with *z*-stack reconstructions show abnormalities in the heart myofibers in *tinC-GFP;tinC>Ras85D^{V12S35}*, *tinC-GFP; tinC>Ras85D^{V12G37}* and *tinC-GFP; tinC>Ras85D^{V12C40}* flies as compared with *tinC-GFP; tinC-Gal4* controls. Scale bar: 50 µm. (G) Fluorescent imaging of nuclear-localized RFP in hearts from *tinC>RFP^{nuc}* control, *tinC>RFP^{nuc}; tinC>Ras85D^{V12S35}*, *tinC>RFP^{nuc}; tinC>Ras85D^{V12G37}* and *tinC>RFP^{nuc}; tinC>Ras85D^{V12C40}* flies. The A2 and A3 abdominal segments are shown.

under the direct control of the cardiac-specific *tinC* genomic element in the context of the *tinC-Gal4* driver (designated *tinC-GFP; tinC-Gal4*). Hearts from *tinC-GFP; tinC-Gal4* flies had circumferentially oriented fibers specifically in cardiomyocytes, and these fibers were readily distinguished from the longitudinal muscle fibers of the dorsal diaphragm (supplementary material Fig. S3). Confocal microscopy and *z*-stack reconstructions of hearts isolated from *tinC-GFP; tinC>EGFR^{Act}* and *tinC-GFP; tinC>Ras85D^{V12}* flies showed abnormal cardiac morphology, with myofiber disarray compared with controls (Fig. 1E,F).

Heart wall thicknesses can increase because of an increase in cardiomyocyte number (hyperplasia), an increase in the size of individual cardiomyocytes (hypertrophy) or a combination of both processes. To distinguish among these possibilities, we engineered transgenic flies that harbored GFP and nuclear-localized RFP under the control of *tinC* (designated *tinC-GFP; tinC>RFP^{nuc}*). Hearts from *tinC-GFP; tinC>RFP^{nuc}/EGFR^{Act}* and *tinC-GFP; tinC>RFP^{nuc}/Ras85D^{V12}* had the same number of cardiomyocytes as controls, indicating that the increased heart wall thickness was the result of cardiomyocyte hypertrophy, not an increase in cell proliferation (Fig. 1G; supplementary material Fig. S4). Because the activation of EGFR and Ras is known to cause cellular proliferation in other tissues and organs, we validated the effects of the *EGFR^{Act}* and *Ras85D^{V12}* transgenes in other tissues and observed

proliferative responses in the wing (data not shown). These findings demonstrate that the cardiac-specific activation of EGFR and the downstream signaling component Ras cause cardiac hypertrophy in the fly. Moreover, the tissue context in which EGFR or Ras is activated dictates different cellular responses that lead to proliferation or hypertrophy.

Ras-mediated cardiac hypertrophy occurs via signals directed to Raf

Ras is a nodal point in signal transduction and directs the activation of multiple, distinct downstream signal molecules. Therefore, we examined the effects of activated Ras mutants that harbor second site mutations in the effector loop and thereby preferentially direct the activation of Raf, RalGDS or phosphatidylinositol-3-kinase (PI3K) signals via *Ras85D^{V12S35}*, *Ras85D^{V12G37}* or *Ras85D^{V12C40}*, respectively (Bergmann et al., 1998; White et al., 1995). OCT measurements revealed that flies that were heterozygous for *tinC>Ras85D^{V12S35}* had smaller EDDs compared with *tinC>Ras85D^{V12G37}*, *tinC>Ras85D^{V12C40}* or control flies (Fig. 2A,B; supplementary material Table S1). Interestingly, flies that were heterozygous for *tinC>Ras85D^{V12C40}* had enlarged EDDs compared with controls (EDD 103.9±5.6 μm for *tinC>Ras85D^{V12C40}*; Fig. 2A,B,D; supplementary material Table S1). Confocal microscopy of hearts isolated from *tinC-GFP; tinC>Ras85D^{V12S35}*
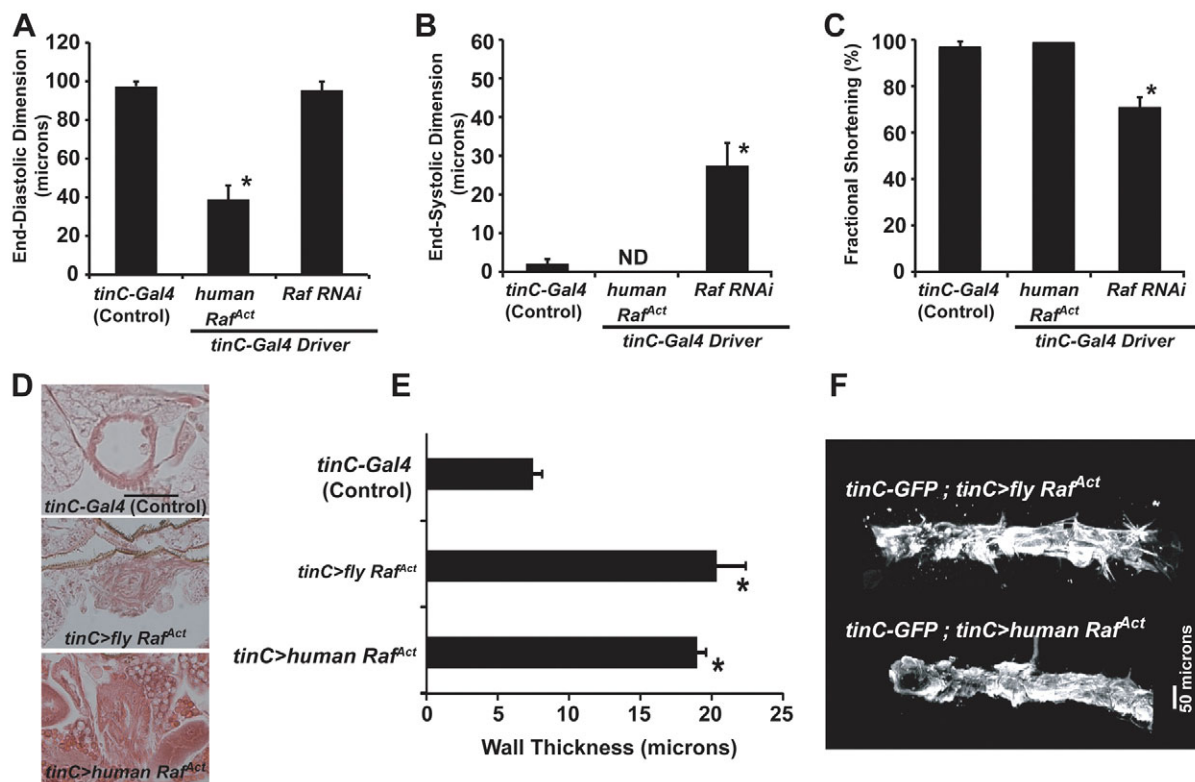

Fig. 3. Activated fly or human Raf causes cardiac hypertrophy. Summary data for OCT measurements of EDD (A), ESD (B) and FS (C) for *tinC-Gal4* driver control (*n*=18), *tinC>human Raf^{Act}* (*n*=18) and *tinC>Raf^{RNAi}* (*n*=12) adult flies. *P<0.05 for indicated transgenic fly line vs control. ND, not detected. (D) Histological sections in transverse orientation showing heart wall thicknesses in the A1/A2 segments from *tinC-Gal4* driver control, *tinC>fly Raf^{Act}* and *tinC>human Raf^{Act}* adult flies. Scale bar: 50 μm. (E) Summary data of wall thicknesses from *tinC-Gal4* driver control (*n*=10), *tinC>fly Raf^{Act}* (*n*=5) and *tinC>human Raf^{Act}* (*n*=3) adult flies. *P<0.05 for indicated transgenic fly line vs control. (F) Confocal microscopy with *z*-stack reconstructions shows abnormalities in the heart myofibers in *tinC-GFP; tinC>fly Raf^{Act}* and *tinC-GFP; tinC>human Raf^{Act}* flies.

flies showed abnormal cardiac morphology compared with hearts isolated from flies expressing $Ras85D^{V12G37}$ or $Ras85D^{V12C40}$, or from controls that contained driver alone (Fig. 2F). Histological analyses demonstrated similar heart wall thicknesses for flies expressing $Ras85D^{V12S35}$ compared with $Ras85D^{V12G37}$ or $Ras85D^{V12C40}$, or with controls (Fig. 2E; supplementary material Table S1). These findings were consistent with observations that, although Ras85D^{V12S35} preferentially signals to Raf, the intensity of Ras85D^{V12S35}-mediated signals is diminished compared with those of Ras85D^{V12} (White et al., 1995). Additionally, hearts from *tinC-GFP; tinC>RFP^{nuc}/Ras85D^{V12S35}* flies, *tinC-GFP; tinC>RFP^{nuc}/Ras85D^{V12G37}* flies and *tinC-GFP; tinC>RFP^{nuc}/Ras85D^{V12C40}* flies had the same number of cardiomyocytes, indicating that each *Ras* transgene did not cause cardiomyocyte proliferation (Fig. 2G).

Activated fly or human Raf causes cardiac hypertrophy and an increase in cardiomyocyte ploidy in adult flies

Next, we examined the effects of cardiac-specific expression of fly and human Raf proteins in the adult fly heart. Fly and human Raf constructs that had deletions of the amino acids from 2 to 431 for fly and from 2 to 334 for human Raf1 (designated fly Raf^{Act} and human Raf^{Act}) have been shown to possess constitutive activity that is independent of Ras (Brand and Perrimon, 1994). Hearts from flies that were heterozygous for *tinC>fly Raf^{Act}* or *tinC>human Raf^{Act}* had smaller EDDs, cardiomyocyte myofiber disarray and increased heart wall thicknesses compared with controls (Figs 3, 4; supplementary material Table S1). Conversely, hearts from flies that were heterozygous for *tinC>Raf^{RNAi}* lines had increased ESDs, decreased fractional shortening (FS) and thinner heart walls compared with controls (Fig. 3B,C; supplementary material Table S1). Additionally, hearts rates, cardiac cycle durations, systolic and diastolic intervals, and arrhythmia indices were similar between control and Raf^{Act} hearts (supplementary material Fig. S5).

Hearts from *tinC-GFP; tinC>RFP^{nuc}/fly Raf^{Act}* and *tinC-GFP; tinC>RFP^{nuc}/human Raf^{Act}* had the same number of cardiomyocytes (Fig. 5A). However, the nuclear RFP signal appeared intense in the hearts expressing Raf^{Act} (Fig. 5A). Because RFP expression was non-quantitative, we performed additional quantitative analyses of cardiomyocyte DNA content using established methods (Fox et al., 2010). Hearts that expressed Raf^{Act} had an increase in cardiomyocyte ploidy [mean ploidy (C value) was 33 for *tinC-GFP; tinC>human Raf^{Act}* flies versus 22 for *tinC-GFP; tinC-Gal4* controls, $P<0.05$], suggesting that the expression of activated human Raf increased endoreplication (Fig. 5B).

To examine whether the observed hypertrophy is largely, or solely, caused by the increase in ploidy of the cells, we used RNAi directed against *Fzr* to artificially decrease polyploidization in the presence of activated Raf. Fzr promotes cell cycle progression during *Drosophila* endocycling in multiple tissues, and postmitotic salivary gland cells fail to enter endoreduplication cycles in Fzr-deficient flies (Sigrist and Lehner, 1997; Zielke et al., 2008). Therefore, we examined the effects of cardiac-specific expression of *Fzr RNAi* in the context of Raf^{Act}. The cardiac-specific expression of *Fzr RNAi* prevented Raf-mediated increases in cardiomyocyte ploidy [mean ploidy (C value) was 40 for *tinC-GFP; tinC>human Raf^{Act}* flies versus 17 for *tinC-GFP; tinC>Raf^{Act} + Fzr RNAi* flies, $P<0.05$; Fig. 5C). Interestingly, heart wall thicknesses were similar between *tinC-GFP; tinC>human Raf^{Act}*
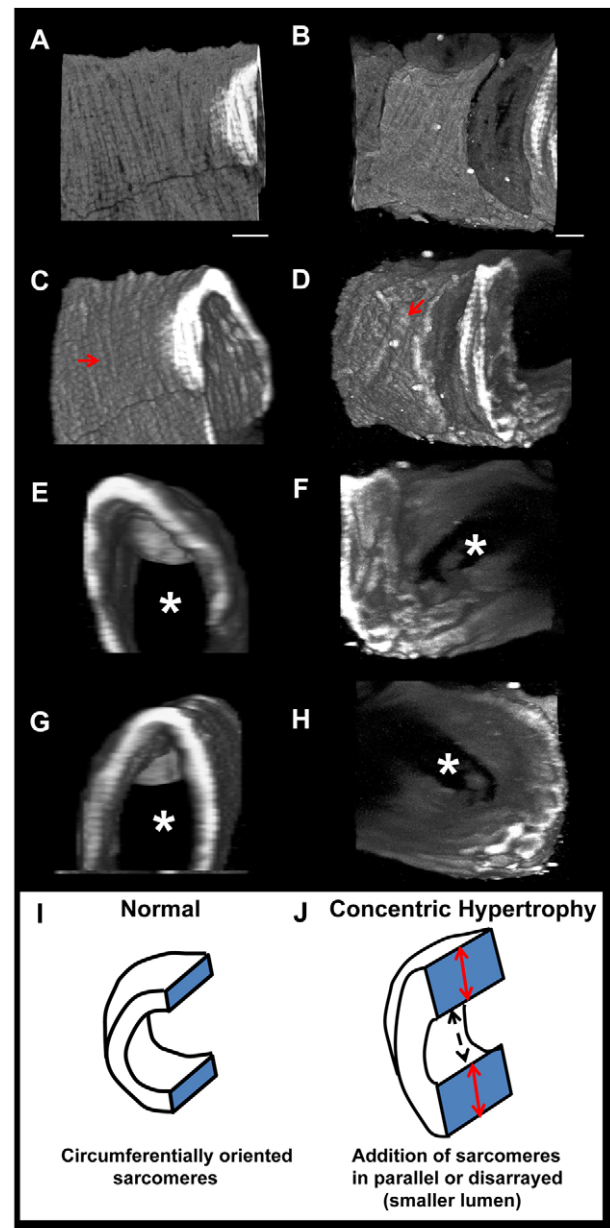

Fig. 4. Raf-mediated changes in cardiomyocyte morphology cause concentric hypertrophy in adult *Drosophila*. Confocal microscopy with *z*-stack reconstruction of the A1/A2 segments of the adult *Drosophila* heart from *tinC-GFP; tinC-Gal4* (A,C,E,G) and *tinC-GFP; tinC>human Raf^{Act}* (B,D,F,H) flies, showing disarrayed fibers and increased thickness in single cardiomyocytes in the latter. Arrows denote the fiber orientations in cardiomyocytes and the asterisks denote the heart lumen. Scale bars: 10 μm. Schematic interpretation of the confocal micrographs showing fly cardiomyocytes that are normal (I) or that have concentric hypertrophy (J).

and *tinC-GFP; tinC>human Raf^{Act} + Fzr RNAi* (Fig. 5D), suggesting that Raf-mediated increases in polyploidy were not required for cardiac hypertrophy.

Because Raf is known to activate MEK, we examined the effects of MEK knockdown in adult fly hearts. Hearts from *tinC>MEK^{RNAi}* flies had slightly increased EDDs, significantly increased ESDs, and
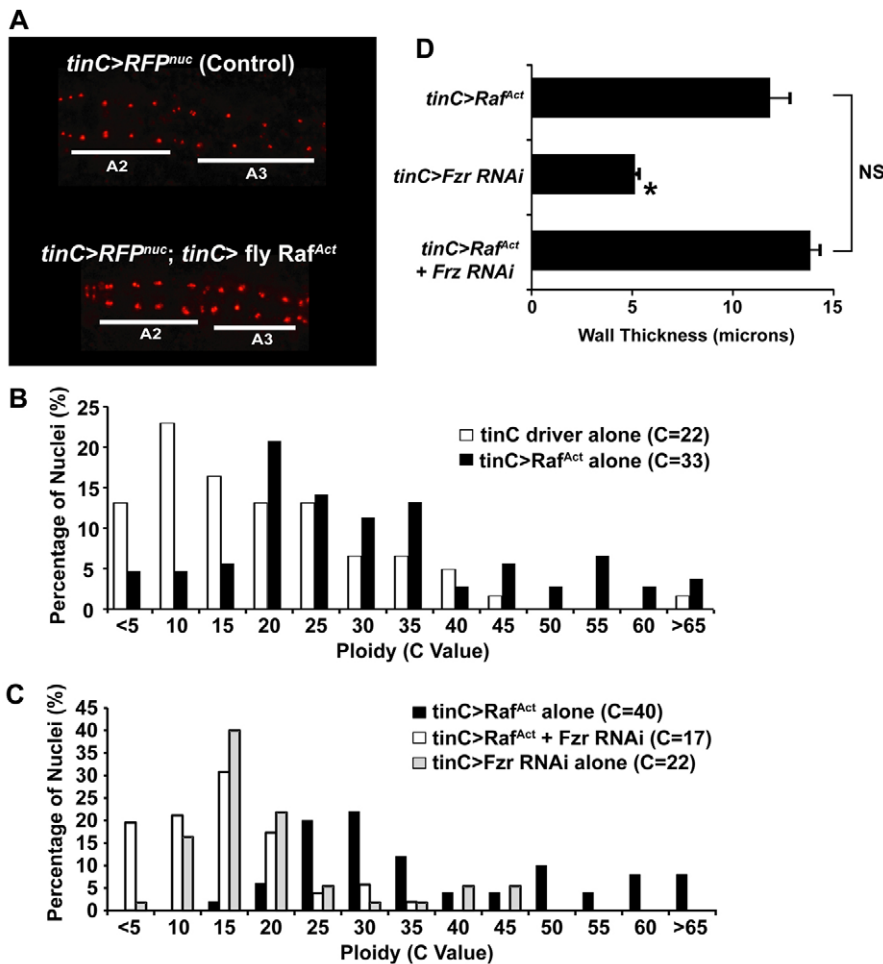
Fig. 5. Raf-mediated cardiac hypertrophy is independent of increases in cardiomyocyte ploidy. (A) Fluorescent imaging of nuclear-localized RFP in hearts from *tinC>RFP^nuc* controls and *tinC>RFP^nuc/fly Raf^Act*. The A2 and A3 abdominal segments are shown. (B) The distribution of cardiomyocyte ploidy (C value) from *tinC-GFP; tinC>human Raf^Act* (*n*=106 nuclei) (black bars) and *tinC-GFP; tinC-Gal4* control (*n*=61 nuclei) hearts (white bars) expressed as the percentage of nuclei of total for each genotype. The mean ploidy C value is shown for each group. *P*<0.05 for *tinC-GFP; tinC>human Raf^Act* versus *tinC-GFP; tinC-Gal4* controls. (C) The distribution of cardiomyocyte ploidy (C value) from *tinC-GFP; tinC>human Raf^Act* (*n*=50 nuclei) (black bars), *tinC-GFP; tinC>human Raf^Act* + *Fzr RNAi* (*n*=52 nuclei) (white bars) and *tinC-GFP; tinC>Fzr RNAi* (*n*=50 nuclei) (gray bars) hearts expressed as the percentage of nuclei of total for each genotype. The mean ploidy C value is shown for each group. (D) Summary data of wall thicknesses from *tinC-GFP; tinC>human Raf^Act* (*n*=6), *tinC-GFP; tinC>human Raf^Act* + *Fzr RNAi* (*n*=6) and *tinC-GFP; tinC>Fzr RNAi* (*n*=5) adult flies. **P*<0.05 for *tinC>human Raf^Act* versus *tinC-GFP; tinC>human Raf^Act* + *Fzr RNAi*. NS, non-significant.

thinner heart walls compared with controls (Fig. 6A-D; Fig. 7; supplementary material Table S1). Flies that had cardiac-specific expression of activated Raf in the context of *MEK^RNAi* (*tinC>MEK^RNAi*, *tinC>human Raf^Act*) had cardiac chamber dimensions, heart wall thicknesses and cardiomyocyte myofibrillar architecture that were similar to *tinC>MEK^RNAi* (Fig. 6A-D; Fig. 7; supplementary material Table S1). Five independent transgenic *UAS-MEK^RNAi* lines were examined, and four lines rescued the Raf-mediated cardiac abnormalities (supplementary material Table S1 and data not shown), suggesting that Raf-dependent signals to MEK are necessary for Raf-mediated cardiac hypertrophy.

ERK is necessary, but not sufficient, for the development of cardiac hypertrophy in adult *Drosophila*

ERK is one of the downstream effector molecules through which Raf mediates cellular signals (Heineke and Molkentin, 2006). Activating mutations in *rolled*, the fly ortholog of *ERK*, were initially identified from fly screens of *EGFR* mutants and subsequently shown to result from a mutation of aspartic acid to asparagine at amino acid 334 (Brunner et al., 1994). The aspartate amino acid at position 334 in fly ERK is conserved across species, including humans, and ERK^D334N was shown to be a dominant mutation in the catalytic domain of the kinase (Oellers and Hafen, 1996). Therefore, we generated transgenic constructs harboring *UAS-*

ERK^D334N and validated the activity of the transgene in the fly eye using a *GMR-Gal4* driver or in the fly wing using a *dpp-Gal4* driver. *GMR>ERK^D334N* had a rough eye phenotype consistent with the initially characterized fly mutant and *dpp>ERK^D334N* had additional veins and clonal expansion of wing epithelium, indicating that the ERK^D334N transgenes encoded functionally active ERK (Fig. 6E,F). Interestingly, the cardiac chamber dimensions and heart wall thicknesses in *tinC>ERK^D334N* were similar to controls (Fig. 6A; Fig. 7A; supplementary material Table S1). Thus, the cardiac-specific expression of activated ERK did not phenocopy the cardiac hypertrophy under conditions of EGFR, Ras or Raf activation. Next, we examined the effects of genetically ablating ERK in the context of activated Raf. *tinC>ERK^RNAi* flies had cardiac parameters that were similar to controls but the heart walls were thinner and had normal-appearing cardiomyocyte myofibrillar structure (Fig. 6A-D; Fig. 7; supplementary material Table S1). Flies with cardiac-specific expression of activated Raf in the context of *ERK^RNAi* (*tinC>ERK^RNAi*, *tinC>human Raf^Act*) had cardiac chamber dimensions, heart wall thicknesses and cardiomyocyte myofibrillar architecture that were similar to *tinC>ERK^RNAi*, suggesting that *ERK* is epistatic to *Raf*. Thus, the activation of ERK did not cause cardiac hypertrophy. However, the inhibition of ERK prevented Raf-mediated cardiac hypertrophy, suggesting that ERK is necessary but not sufficient (Fig. 8).
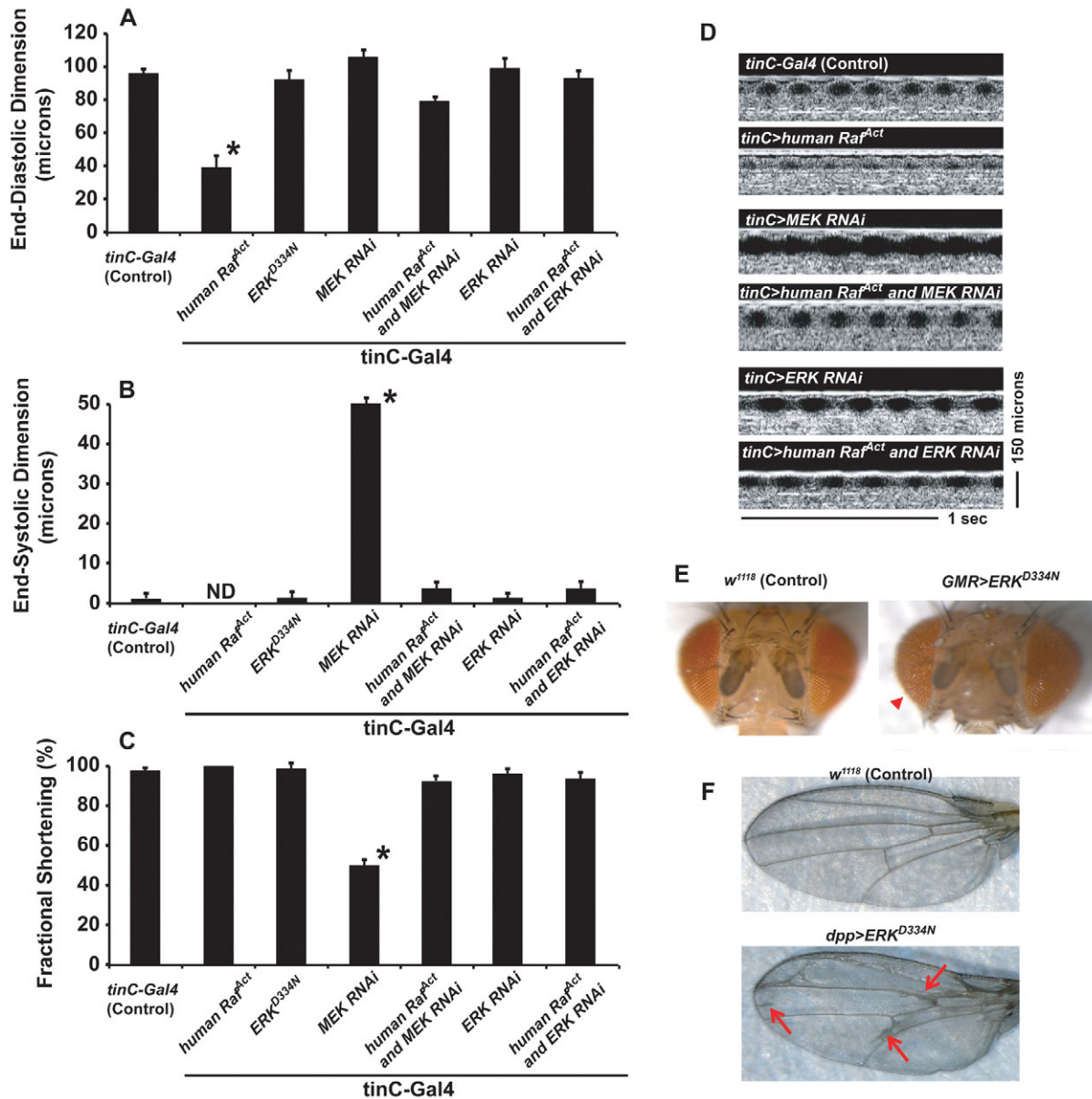
Fig. 6. The inhibition of MEK or ERK prevents Raf-mediated cardiac dysfunction. Summary data for OCT measurements of EDD (A), ESD (B) and FS (C) for *tinC-Gal4* driver controls (*n*=18), *tinC>human Raf^Act* (*n*=18), *tinC>ERK^D334N* (*n*=11), *tinC>MEK^RNAi* (*n*=12), *tinC>human Raf^Act* with *MEK^RNAi* (*n*=15), *tinC>ERK^RNAi* (*n*=15) and *tinC>human Raf^Act* with *ERK^RNAi* (*n*=15). **P*<0.05 for indicated transgenic fly line vs control. (D) Representative M-mode OCT images for *tinC-Gal4* driver controls, *tinC>human Raf^Act*, *tinC>MEK^RNAi*, *tinC>human Raf^Act* with *MEK^RNAi*, *tinC>ERK^RNAi* and *tinC>human Raf^Act* with *ERK^RNAi*. A 1-second marker and 150 μm standard are shown. (E) Expression of ERK^D334N in the fly eye using a *GMR-Gal4* driver causes a rough eye phenotype (arrowhead). (F) Expression of ERK^D334N in the wing using a *dpp-Gal4* driver causes clonal expansion of wing epithelium (arrows).

DISCUSSION

The inhibition of EGF ligand or EGFR by dominant-negative EGFR molecules results in enlarged cardiac chambers in adult flies (Yu et al., 2010). Our current studies show that the cardiac-specific expression of activated EGFR, Ras or Raf (human or fly) causes decreased heart chamber lumens. These results raise the question: how does the lumen of a heart composed of pairs of single myocytes undergo reduction or enlargement (i.e. dilation)? One proposed explanation is that molecular signals that drive the addition of sarcomeres added in series produce an eccentric hypertrophy and resultant enlarged heart lumen. Conversely, signals that promote either the addition of sarcomeres in parallel or myofiber disarray produce enlarged myocytes and resultant concentric hypertrophy in the fly. This explanation is consistent with a model proposed by Molkentin's group that showed that ERKs regulate the balance between eccentric and concentric cardiac growth in mammals (Kehat et al., 2011). Transgenic mice that had genetically ablated ERK1 and ERK2 in the heart (*Erk1^−/−*, *Erk2^fl/flαMHC-Cre* mice) developed an eccentric hypertrophy, and isolated cardiomyocytes from these mice displayed elongation. Our
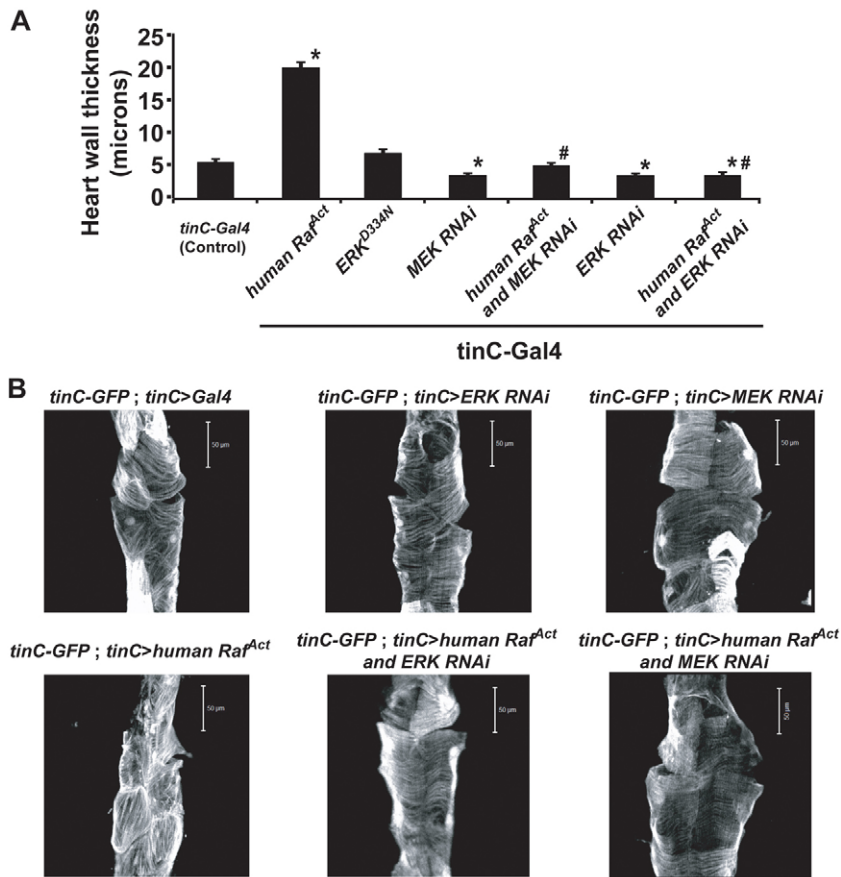
A

B

Fig. 7. The inhibition of MEK or ERK prevents Raf-mediated cardiac hypertrophy. (A) Summary data of wall thicknesses for *tinC-Gal4* driver controls (*n*=10), *tinC>human Raf^Act* (*n*=3), *tinC>ERK^D334N* (*n*=8), *tinC>MEK^RNAi* (*n*=4), *tinC>human Raf^Act* with *MEK^RNAi* (*n*=6), *tinC>ERK^RNAi* (*n*=4) and *tinC>human Raf^Act* with *ERK^RNAi* (*n*=4). *$P<0.05$ for indicated stock versus control. #, $P<0.05$ for indicated stock versus *tinC>human Raf^Act*. (B) Confocal microscopy with *z*-stack reconstructions showing heart myofibers in *tinC-GFP; tinC-Gal4* controls, *tinC-GFP; tinC>human Raf^Act*, *tinC-GFP; tinC>ERK^RNAi*, *tinC-GFP; tinC>MEK^RNAi*, *tinC-GFP; tinC>human Raf^Act* with *MEK^RNAi* and *tinC-GFP; tinC>human Raf^Act* with *ERK^RNAi*. Scale bars: 50 µm.

results show that the inhibition of ERK or MEK causes a thinner cardiomyocyte and in some cases an enlargement in EDDs, consistent with findings in mammalian models.

The expression of activated EGFR, Ras or Raf promotes cell proliferation in the eye or wing (Baker and Rubin, 1989; Brunner et al., 1994; Halfon et al., 2000; Karim and Rubin, 1998; Lu et al., 1994). The activation of these pathway components in the fly heart caused cardiac hypertrophy. We observed myocyte polyploidy in control hearts and increases in myocyte ploidy in the Raf^Act hearts that is suggestive of incomplete endocycling, repetitive rounds of genome replication. An increase in cell ploidy is achieved through endoreplication, in which genomic DNA content increases without cellular division (Lee et al., 2009). Endoreplication is a common occurrence among species and, in the fly, some cells can have up to 2048 copies of the euchromatic genome (Edgar and Orr-Weaver, 2001). This process has been described as an effective strategy for cell growth, often found in differentiated cells that are large or have high metabolic activity.

Prior studies have shown changes in cardiomyocyte DNA content, ploidy level and nuclear number in mammalian hearts across multiple species, including humans (Adler et al., 1996). Post-mortem examinations of human hearts demonstrated that the degree of polyploidy closely correlated with myocardial hypertrophy (Adler and Friedburg, 1986; Sandritter and Scomazzoni, 1964). Recently, endoreduplication has been observed in mouse cardiomyocytes after cardiac injury (Hesse et al., 2012). Augmented endoreplication, and an increase in ploidy, might

represent a mechanism by which cells can adapt to high metabolic demands (Edgar and Orr-Weaver, 2001). Therefore, growth conditions or stimuli that promote cardiac hypertrophy might cause the myocyte to adapt by increasing ploidy, thereby providing more copies of essential genes required to respond to these cues (Ahuja et al., 2007).

In our studies, *Fzr RNAi* prevented Raf-mediated increases in cardiomyocyte ploidy. Interestingly, the cardiac-specific expression of *Fzr RNAi* did not significantly change the degree of Raf-mediated cardiac hypertrophy. Therefore, the cardiac hypertrophy observed in the context of activated Raf does not require increased polyploidization. One interpretation of these findings is that the signals emanating from Raf bifurcate towards two distinct pathways: one that drives DNA replication and one that promotes cardiac hypertrophy.

The results further support the concept that the cellular context in which signaling molecules are expressed defines the cell growth response, namely hyperplasia or hypertrophy. During fly development, signals from EGFR are required for the specification and diversification of embryonic muscle progenitors, including cardiac cells (Baylies et al., 1998; Bodmer and Venkatesh, 1998; Carmena et al., 1995; Zaffran and Frasch, 2002). Somatic muscles and the cardiac cells develop from specialized progenitors (Carmena et al., 1995; Carmena et al., 1998; Ward and Skeath, 2000). Each progenitor cell divides asymmetrically and produces two founder cells that specify individual muscle cell fates and give rise to multinucleate myofibers (Rushton et al., 1995). Michelson's group
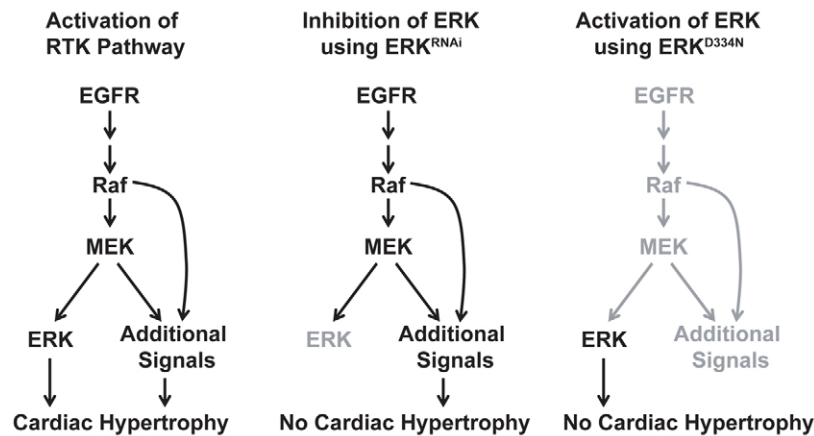
Fig. 8. Activated ERK is necessary, but not sufficient, for Raf-mediated cardiac hypertrophy in adult *Drosophila*. The EGFR-mediated activation of Raf results in the activation of ERK and additional signals that lead to cardiac hypertrophy. The inhibition of ERK via cardiac-specific ERK[RNAi] prevents Raf-mediated cardiac hypertrophy. However, the cardiac-specific expression of ERK[D334N] does not, by itself, produce cardiac hypertrophy.

has shown that hyperactive EGFR, using early mesodermal *GAL4* drivers including *twist-GAL4* or *24B-GAL4*, generates supernumerary mesodermal founder cells and causes a duplication of dorsal acute muscle 1 (DA1), a larval body wall muscle (Buff et al., 1998). Moreover, Wingless and the TGFβ family member Decapentaplegic, two members of the signals from the Wnt family, prepattern the mesoderm and render cells competent to respond to Ras-MAPK activation (Halfon et al., 2000). Thus, the timing of EGFR and Ras signals during development and the integration of cellular cues dictates the response of myocytes, including the cardiomyocytes.

We used the cardiac driver *tinC-Gal4*, which is expressed later in mesodermal development: this might explain why we did not observe the increase in cardiomyocytes that has been observed with drivers that are expressed earlier in mesodermal development (Lo and Frasch, 2001; Zaffran et al., 2006). Our findings suggest that adult *Drosophila* cardiomyocytes lose the ability to proliferate when EGFR signals are activated after cardiomyocyte differentiation, similar to observations in mammals. Whether this lack of myocyte proliferation is specific to EGFR, Ras and Raf or is more generalizable to other stimuli remains to be investigated.

In mice, the indirect activation of ERKs via upstream signaling molecules has been shown to cause cardiac hypertrophy. Transgenic knock-in mice expressing Raf[L613V], a mutation that is associated with Noonan syndrome, develop cardiac hypertrophy through the activation of the MEK-ERK pathway (Wu et al., 2011). The cardiac-specific expression of MEK produces concentric hypertrophy attributed to the activation of ERK (Bueno et al., 2000). The homozygous deletion of ERK1 prevents valvular abnormalities caused by selective overexpression of an activated mutant of protein tyrosine phosphatase, non-receptor type 11 (Shp2[Q79R]) in the developing endocardial cushions (Krenz et al., 2008). However, studies of the cardiac-specific expression of activated transgenic ERKs on cardiac hypertrophy are lacking. Thus, these prior studies cannot rule out ERK-independent signals that contribute to Raf-mediated cardiac hypertrophy.

Our findings suggest that the activation of ERK is necessary, but not sufficient, for the development of Raf-mediated cardiac hypertrophy. This suggests that ERK-independent signals emanating from Raf function in concert with ERK to produce cardiac hypertrophy (Fig. 8). Alternatively, the mutation in

ERK[D334N] might differentially influence downstream effector molecules that promote cell proliferation in tissues receptive to cell cycle progression (i.e. the eye and wing) but do not produce a growth response in the fly heart. Alternatively, the inability of ERK[D334N] to produce cardiac hypertrophy might be explained by the degree to which this allele is 'activated' such that it might suffice to cause visible effects in the eyes and wings but perhaps be insufficient for producing effects in the heart. In either case, our fly model could provide a means to identify ERK-independent signals that promote hypertrophy or are differentially regulated to control cell proliferation and growth in different tissues.

MATERIALS AND METHODS
Stocks/transgenics
The p{tinC-GFP} ; p{tinC- Gal4} stocks were derived from p{tinC-GFP} and p{tinC-Gal4} stocks as previously described (Wolf et al., 2006; Yu et al., 2010). p{UAS-Ras85D[V12C40]} and p{UAS-ERK[D334N]} were engineered by site-directed mutagenesis from cDNA from w[1118], and transgenic insertion lines were obtained by standard protocols (Brand and Perrimon, 1993). p{tinC-GFP} ; p{UAS-RFP[NUC]},p{tinC-Gal4} were generated using p{tinC-GFP} ; p{tinC-Gal4} and p{UAS-RFP[NUC]} transgenic stocks. Transgenic flies harboring p{UAS-Ras85D[V12S35]} and p{UAS-Ras85D[V12G37]} were kindly provided by Hermann Steller (Bergmann et al., 1998). p{tinC-GFP} ; p{tinC-Gal4} or p{tinC-GFP};p{UAS[RFPNUC]},p{tinC-Gal4} were used to drive p{UAS-transgenes} in the experiments.

The Vienna Drosophila RNAi Center (VDRC) RNAi stock directed against Fzr (w[1118]; P{GD9960}v25550) was kindly provided by Don Fox (Duke University, Durham, NC). All other fly stocks were obtained from the Bloomington Stock Center or the Transgenic RNAi Project (TRiP) at Harvard Medical School (http://www.flyrnai.org/). All fly stocks were maintained on standard yeast protein media at room temperature (Ashburner et al., 2005).

OCT measurement of cardiac function in adult *Drosophila*
Cardiac function in adult *Drosophila* was measured using a custom built OCT microscopy system (Bioptigen Inc., Durham, NC) as previously described (Wolf et al., 2006; Yu et al., 2010). Adult female *Drosophila* between 3 and 10 days post-eclosion were briefly subjected to CO_2, placed on a soft gel support, and allowed to fully awaken based on body movement. All flies were imaged in B-modes

in the longitudinal orientation to identify the cardiac chamber in the A1 segment and then in the transverse orientation to center the heart chamber. Multiple 3-second OCT M-modes were recorded for each fly. M-mode OCT images were processed using ImageJ software and referenced to a 150-μm standard. After M-modes were acquired, the flies were re-examined in the transverse B-mode orientation to assure consistent measurements from the heart chamber. End-diastolic dimensions (EDDs), end-systolic dimensions (ESDs) and heart rate were determined from three consecutive heart beats. Fractional shortening (FS) was calculated as (EDD−ESD)/EDD×100.

Histological analysis

Fly heart wall thicknesses were measured as previously described (Yu et al., 2010). Briefly, adult female flies of 5-7 days age after eclosion were collected and fixed in Telly's fixation buffer (60% ethanol, 3.33% formalin, 4% glacial acetic acid) for at least 1 week at 4°C. Previously, we determined that cardiac chamber sizes in flies from this fixation step were similar to the EDD in awake, adult flies as assessed using OCT. Adult *tinC>EGFR^{Act}* and *tinC>Ras85D^{V12}* flies were collected at 2-3 days after eclosion because they had impaired survival.

Specimens were dehydrated in ethanol through sequential gradients. Then, the samples were washed twice with xylenes before immersion in liquid paraffin. After solidification, paraffin blocks were sectioned serially at 8 μm thickness in longitudinal or transverse orientation. Sections were rehydrated and stained with hematoxylin and eosin. Established criteria were used to control for the position of the heart chamber among different flies that were evaluated (Yu et al., 2010). Measurements were made in three serial 8-μm sections. Sections were analyzed using a Leica DM2500 microscope equipped with a Leica DFC310FX digital camera. Wall thickness was calculated by measuring the cardiac chamber wall width along the mid-dorsal, mid-ventral, left lateral and right lateral wall in three serial sections to obtain the mean ± s.e.m.

Evaluation of adult cardiac morphology

Adult *Drosophila* corresponding to the F1 offspring of *p{tinC-GFP}* ; *p{tinC- Gal4}* stocks crossed to specific *p{UAS-transgenes}* or *w^{1118}* (controls) were collected at 2-3 days age, post-eclosion, to examine adult cardiac morphology. Flies were briefly anesthetized by administration of CO_2, the head and thorax were removed and the abdomen was placed in artificial hemolymph buffer [108 mM Na$^+$, 5 mM K$^+$, 2 mM Ca^{2+}, 8 mM MgCl$_2$, 1 mM NaH$_2$PO$_4$, 4 mM NaHCO$_3$, 10 mM sucrose, 5 mM trehalose, and 5 mM HEPES (pH 7.1)]. An incision was made along the ventral aspect of the abdomen and the internal abdominal organs were gently removed. The surrounding fat and tissue were removed using a pulled glass capillary pipette. Hemolymph buffer that contained 10 mM EGTA was then added to relax the cardiac muscle as described by Alayari et al. (Alayari et al., 2009). Next, samples were fixed in 4% paraformaldehyde for 20 minutes at room temperature prior to staining with a primary anti-GFP-antibody (1:500; Invitrogen, Inc.) and secondary antibody conjugated to Alexa Fluor 488 (1:500; Invitrogen, Inc.) for detection of cardiomyocytes, with phalloidin–Texas-Red (1:1000; Invitrogen, Inc.) for actin staining, and with TO-PRO-3 (1:10,000; Invitrogen, Inc.) for DNA staining. The stained heart preparations were visualized under a Zeiss

LSM510 confocal microscope and 0.4 μm *z*-stack images were analyzed.

For evaluation of cardiac morphology during pupal stages, *Drosophila* corresponding to the F1 offspring of *p{tinC-GFP}* ; *p{tinC- Gal4}* stocks crossed to specific *p{UAS-transgenes}* or *w^{1118}* (controls) were collected between the ~P6 and P13 stages according to staging described by Bainbridge and Bownes (Bainbridge and Bownes, 1981). Pupal hearts were directly visualized using a Leica M165FC fluorescent stereomicroscope. For embryo staining, pericardin was detected using EC11 anti-Pericardin-5. The EC11 anti-Pericardin-5 developed by D. Gratecos was obtained from the Developmental Studies Hybridoma Bank (DSHB), developed under the auspices of the NICHD and maintained by The University of Iowa, Department of Biology, Iowa City, IA.

Evaluation of adult cardiomyocyte ploidy

Ploidy was determined by adapting methods previously described (Fox et al., 2010). Adult *Drosophila* corresponding to the F1 offspring of *p{tinC-GFP}* ; *p{tinC-Gal4}* stocks crossed to specific *p{UAS-transgenes}* or *w^{1118}* (controls) were collected at 2-3 days age, post-eclosion, and hearts were dissected in artificial hemolymph buffer as described above. Testes from adult male files were isolated as internal controls because this tissue is haploid. Dissected hearts were then removed from the cuticles. Hearts and testes were placed on the same coverslip for all subsequent steps. Samples were fixed in 4% paraformaldehyde at room temperature for 20 minutes, then washed three times (1 minute per wash) in TBT buffer (10 mM Tris-HCl pH 8.0, 250 mM NaCl, 0.1% BSA, 0.1% Triton X-100) prior to staining nuclei with TO-PRO-3 (1:5000 dilution in TBT) for 20 minutes at room temperature in the dark. Samples were then washed three times (1 minute per wash) in TBT prior to adding VECTASHIELD, applying a positively charged glass slide (Sigma) and squashing the slide for 10 seconds. The samples were then analyzed by obtaining *z*-stacks of TO-PRO-3-stained nuclei using confocal microscopy. Cardiomyocytes were identified by live GFP expression. Identical emission intensities were used for each slide to quantify TO-PRO-3 staining of myocyte and testis nuclei. The intensity of each myocyte or testis nuclei was quantified using ImageJ, and myocyte nuclei TO-PRO-3 expression was normalized to testis nuclei TO-PRO-3 expression for each slide to calculate ploidy. Ploidy was expressed as the C-value, where a C-value of 1 refers to the amount of DNA contained within a haploid nucleus.

Heart rate analyses

Adult *Drosophila* corresponding to the F1 offspring of *p{tinC-GFP}* ; *p{tinC-Gal4}* stocks crossed to specific *p{UAS-human Raf^{Act}}* or *w^{1118}* (controls) were collected at 2-3 days age, post-eclosion, and hearts were dissected in artificial hemolymph buffer as described above. Heart movements were recoded using a Leica GPF stereoscope equipped with an Andor iXon X3 EMCCD camera at a rate of 100 frames per second for 10 seconds and processed using Solaris software (Andor, Inc.). Each recording was processed using Excel software to identify the local minima and maxima and corresponding time-stamped image frame. The systolic interval (SI), diastolic interval (DI), RR (peak-to-peak interval), CC (cardiac cycle length), fraction of cardiac cycle in systole (SI/CC), fraction of cardiac cycle in diastole (DI/CC), and the arrhythmia index (AI)

are shown. AI was calculated as the standard deviation of the RR interval normalized to the median of the RR interval as previously described (Fink et al., 2009).

Statistical analysis

Comparisons of EDD chamber dimensions were determined by either a Student's *t*-test for two samples or an analysis of variances (ANOVA) with corrections for multiple comparisons when necessary. GraphPad Prism (GraphPad Software, Inc.) and Microsoft Excel statistical software were used for all analyses.

REFERENCES

Adler, C. P. and Friedburg, H. (1986). Myocardial DNA content, ploidy level and cell number in geriatric hearts: post-mortem examinations of human myocardium in old age. *J. Mol. Cell. Cardiol.* **18**, 39-53.

Adler, C. P., Friedburg, H., Herget, G. W., Neuburger, M. and Schwalb, H. (1996). Variability of cardiomyocyte DNA content, ploidy level and nuclear number in mammalian hearts. *Virchows Arch.* **429**, 159-164.

Ahuja, P., Sdek, P. and MacLellan, W. R. (2007). Cardiac myocyte cell cycle control in development, disease, and regeneration. *Physiol. Rev.* **87**, 521-544.

Alayari, N. N., Vogler, G., Taghli-Lamallem, O., Ocorr, K., Bodmer, R. and Cammarato, A. (2009). Fluorescent labeling of Drosophila heart structures. *J. Vis. Exp.* **32**, e1423.

Ashburner, M., Golic, K. G. and Hawley, R. S. (2005). *Drosophila: a Laboratory Handbook*. Cold Spring Harbor, NY: Cold Spring Harbor Laboratory Press.

Bainbridge, S. P. and Bownes, M. (1981). Staging the metamorphosis of Drosophila melanogaster. *J. Embryol. Exp. Morphol.* **66**, 57-80.

Baker, N. E. and Rubin, G. M. (1989). Effect on eye development of dominant mutations in Drosophila homologue of the EGF receptor. *Nature* **340**, 150-153.

Baylies, M. K., Bate, M. and Ruiz Gomez, M. (1998). Myogenesis: a view from Drosophila. *Cell* **93**, 921-927.

Bergmann, A., Agapite, J., McCall, K. and Steller, H. (1998). The Drosophila gene hid is a direct molecular target of Ras-dependent survival signaling. *Cell* **95**, 331-341.

Bodmer, R. and Venkatesh, T. V. (1998). Heart development in Drosophila and vertebrates: conservation of molecular mechanisms. *Dev. Genet.* **22**, 181-186.

Brand, A. H. and Perrimon, N. (1993). Targeted gene expression as a means of altering cell fates and generating dominant phenotypes. *Development* **118**, 401-415.

Brand, A. H. and Perrimon, N. (1994). Raf acts downstream of the EGF receptor to determine dorsoventral polarity during Drosophila oogenesis. *Genes Dev.* **8**, 629-639.

Braunwald, E. and Bonow, R. O. (2012). *Braunwald's Heart Disease: a Textbook of Cardiovascular Medicine*. Philadelphia, PA: Elsevier/Saunders.

Brunner, D., Oellers, N., Szabad, J., Biggs, W. H., III, Zipursky, S. L. and Hafen, E. (1994). A gain-of-function mutation in Drosophila MAP kinase activates multiple receptor tyrosine kinase signaling pathways. *Cell* **76**, 875-888.

Bueno, O. F., De Windt, L. J., Tymitz, K. M., Witt, S. A., Kimball, T. R., Klevitsky, R., Hewett, T. E., Jones, S. P., Lefer, D. J., Peng, C. F. et al. (2000). The MEK1-ERK1/2 signaling pathway promotes compensated cardiac hypertrophy in transgenic mice. *EMBO J.* **19**, 6341-6350.

Buff, E., Carmena, A., Gisselbrecht, S., Jiménez, F. and Michelson, A. M. (1998). Signalling by the Drosophila epidermal growth factor receptor is required for the specification and diversification of embryonic muscle progenitors. *Development* **125**, 2075-2086.

Carmena, A., Bate, M. and Jiménez, F. (1995). Lethal of scute, a proneural gene, participates in the specification of muscle progenitors during Drosophila embryogenesis. *Genes Dev.* **9**, 2373-2383.

Carmena, A., Murugasu-Oei, B., Menon, D., Jiménez, F. and Chia, W. (1998). Inscuteable and numb mediate asymmetric muscle progenitor cell divisions during Drosophila myogenesis. *Genes Dev.* **12**, 304-315.

Chen, M. H., Kerkelä, R. and Force, T. (2008). Mechanisms of cardiac dysfunction associated with tyrosine kinase inhibitor cancer therapeutics. *Circulation* **118**, 84-95.

Chu, T. F., Rupnick, M. A., Kerkela, R., Dallabrida, S. M., Zurakowski, D., Nguyen, L., Woulfe, K., Pravda, E., Cassiola, F., Desai, J. et al. (2007). Cardiotoxicity associated with tyrosine kinase inhibitor sunitinib. *Lancet* **370**, 2011-2019.

Crone, S. A., Zhao, Y. Y., Fan, L., Gu, Y., Minamisawa, S., Liu, Y., Peterson, K. L., Chen, J., Kahn, R., Condorelli, G. et al. (2002). ErbB2 is essential in the prevention of dilated cardiomyopathy. *Nat. Med.* **8**, 459-465.

Edgar, B. A. and Orr-Weaver, T. L. (2001). Endoreplication cell cycles: more for less. *Cell* **105**, 297-306.

Fink, M., Callol-Massot, C., Chu, A., Ruiz-Lozano, P., Izpisua Belmonte, J. C., Giles, W., Bodmer, R. and Ocorr, K. (2009). A new method for detection and quantification of heartbeat parameters in Drosophila, zebrafish, and embryonic mouse hearts. *Biotechniques* **46**, 101-113.

Fox, D. T., Gall, J. G. and Spradling, A. C. (2010). Error-prone polyploid mitosis during normal Drosophila development. *Genes Dev.* **24**, 2294-2302.

Gelb, B. D. and Tartaglia, M. (2011). RAS signaling pathway mutations and hypertrophic cardiomyopathy: getting into and out of the thick of it. *J. Clin. Invest.* **121**, 844-847.

Halfon, M. S., Carmena, A., Gisselbrecht, S., Sackerson, C. M., Jiménez, F., Baylies, M. K. and Michelson, A. M. (2000). Ras pathway specificity is determined by the integration of multiple signal-activated and tissue-restricted transcription factors. *Cell* **103**, 63-74.

Heineke, J. and Molkentin, J. D. (2006). Regulation of cardiac hypertrophy by intracellular signalling pathways. *Nat. Rev. Mol. Cell Biol.* **7**, 589-600.

Hesse, M., Raulf, A., Pilz, G. A., Haberlandt, C., Klein, A. M., Jabs, R., Zaehres, H., Fügemann, C. J., Zimmermann, K., Trebicka, J. et al. (2012). Direct visualization of cell division using high-resolution imaging of M-phase of the cell cycle. *Nat. Commun.* **3**, 1076.

Karim, F. D. and Rubin, G. M. (1998). Ectopic expression of activated Ras1 induces hyperplastic growth and increased cell death in Drosophila imaginal tissues. *Development* **125**, 1-9.

Kehat, I., Davis, J., Tiburcy, M., Accornero, F., Saba-El-Leil, M. K., Maillet, M., York, A. J., Lorenz, J. N., Zimmermann, W. H., Meloche, S. et al. (2011). Extracellular signal-regulated kinases 1 and 2 regulate the balance between eccentric and concentric cardiac growth. *Circ. Res.* **108**, 176-183.

Krenz, M., Gulick, J., Osinska, H. E., Colbert, M. C., Molkentin, J. D. and Robbins, J. (2008). Role of ERK1/2 signaling in congenital valve malformations in Noonan syndrome. *Proc. Natl. Acad. Sci. USA* **105**, 18930-18935.

Lee, H. O., Davidson, J. M. and Duronio, R. J. (2009). Endoreplication: polyploidy with purpose. *Genes Dev.* **23**, 2461-2477.

Lo, P. C. and Frasch, M. (2001). A role for the COUP-TF-related gene seven-up in the diversification of cardioblast identities in the dorsal vessel of Drosophila. *Mech. Dev.* **104**, 49-60.

Lu, X., Melnick, M. B., Hsu, J. C. and Perrimon, N. (1994). Genetic and molecular analyses of mutations involved in Drosophila raf signal transduction. *EMBO J.* **13**, 2592-2599.

Oellers, N. and Hafen, E. (1996). Biochemical characterization of rolledSem, an activated form of Drosophila mitogen-activated protein kinase. *J. Biol. Chem.* **271**, 24939-24944.

Pandit, B., Sarkozy, A., Pennacchio, L. A., Carta, C., Oishi, K., Martinelli, S., Pogna, E. A., Schackwitz, W., Ustaszewska, A., Landstrom, A. et al. (2007). Gain-of-function RAF1 mutations cause Noonan and LEOPARD syndromes with hypertrophic cardiomyopathy. *Nat. Genet.* **39**, 1007-1012.

Roger, V. L., Go, A. S., Lloyd-Jones, D. M., Adams, R. J., Berry, J. D., Brown, T. M., Carnethon, M. R., Dai, S., de Simone, G., Ford, E. S. et al. (2011). Heart disease and stroke statistics – 2011 update: a report from the American Heart Association. *Circulation* **123**, e18-e209.

Rushton, E., Drysdale, R., Abmayr, S. M., Michelson, A. M. and Bate, M. (1995). Mutations in a novel gene, myoblast city, provide evidence in support of the founder cell hypothesis for Drosophila muscle development. *Development* **121**, 1979-1988.

Sandritter, W. and Scomazzoni, G. (1964). DNA content (feulgen photometry) and dry weight (interference microscopy) of normal and hypertrophic heart muscle fibers. *Nature* **202**, 100-101.

Sigrist, S. J. and Lehner, C. F. (1997). Drosophila fizzy-related down-regulates mitotic cyclins and is required for cell proliferation arrest and entry into endocycles. *Cell* **90**, 671-681.

Suter, T. M., Procter, M., van Veldhuisen, D. J., Muscholl, M., Bergh, J., Carlomagno, C., Perren, T., Passalacqua, R., Bighin, C., Klijn, J. G. et al. (2007). Trastuzumab-associated cardiac adverse effects in the herceptin adjuvant trial. *J. Clin. Oncol.* **25**, 3859-3865.

Vasan, R. S., Larson, M. G., Benjamin, E. J., Evans, J. C. and Levy, D. (1997). Left ventricular dilatation and the risk of congestive heart failure in people without myocardial infarction. *N. Engl. J. Med.* **336**, 1350-1355.

Ward, E. J. and Skeath, J. B. (2000). Characterization of a novel subset of cardiac cells and their progenitors in the Drosophila embryo. *Development* **127**, 4959-4969.

White, M. A., Nicolette, C., Minden, A., Polverino, A., Van Aelst, L., Karin, M. and Wigler, M. H. (1995). Multiple Ras functions can contribute to mammalian cell transformation. *Cell* **80**, 533-541.

Wolf, M. J. (2012). Modeling dilated cardiomyopathies in Drosophila. *Trends Cardiovasc. Med.* **22**, 55-61.

Wolf, M. J. and Rockman, H. A. (2011). Drosophila, genetic screens, and cardiac function. *Circ. Res.* **109**, 794-806.

Wolf, M. J., Amrein, H., Izatt, J. A., Choma, M. A., Reedy, M. C. and Rockman, H. A. (2006). Drosophila as a model for the identification of genes causing adult human heart disease. *Proc. Natl. Acad. Sci. USA* **103**, 1394-1399.

Wu, X., Simpson, J., Hong, J. H., Kim, K. H., Thavarajah, N. K., Backx, P. H., Neel, B. G. and Araki, T. (2011). MEK-ERK pathway modulation ameliorates disease phenotypes in a mouse model of Noonan syndrome associated with the Raf1(L613V) mutation. *J. Clin. Invest.* **121**, 1009-1025.

Yu, L., Lee, T., Lin, N. and Wolf, M. J. (2010). Affecting Rhomboid-3 function causes a dilated heart in adult Drosophila. *PLoS Genet.* **6**, e1000969.

Zaffran, S. and Frasch, M. (2002). Early signals in cardiac development. *Circ. Res.* **91**, 457-469.

Zaffran, S., Reim, I., Qian, L., Lo, P. C., Bodmer, R. and Frasch, M. (2006). Cardioblast-intrinsic Tinman activity controls proper diversification and differentiation of myocardial cells in Drosophila. *Development* **133**, 4073-4083.

Zielke, N., Querings, S., Rottig, C., Lehner, C. and Sprenger, F. (2008). The anaphase-promoting complex/cyclosome (APC/C) is required for rereplication control in endoreplication cycles. *Genes Dev.* **22**, 1690-1703.